MOLEKUL
eISSN: 2503-0310

Articles
https://doi.org/10.20884/1.jm.2026.21.2.7390

Hollow Fiber Imprinted Membranes Cellulose Acetate Based for Hemodialysis

Muhammad Cholid Djunaidi[1]*, Didik Setiyo Widodo[1], Fathimatuz Zahra[1], Nesti Dwi Maharani[1], Heru Susanto[2], Abdullah Malik Islam Filardli[2]

[1] Department of Chemistry, Faculty of Science and Mathematics, Diponegoro University, Semarang, 50275, Indonesia
[2] Department of Chemical Engineering, Faculty of Engineering, Diponegoro University, Semarang, 50275, Indonesia

*Corresponding author email: choliddjunaidi@live.undip.ac.id

Received January 25, 2023; **Accepted** June 24, 2026; **Available online** July 20, 2026

ABSTRACT. One of the important roles of the kidneys is to excrete the residues of the body's metabolism, for example urea, uric acid, and creatinine. If these metabolic residues are allowed to accumulate, they can become toxic to the body, especially the kidneys. Hemodialysis has a process related to the disposal of metabolic residue particles in artificial kidneys which currently use a membrane that functions as a separator for metabolic residues with the patient's blood which is then circulated on its own. This study used Molecularly Imprinted Membrane (MIM) and Non-Imprinted Membrane (NIM) with cellulose and cellulose acetate polymers. The results of this study, the cellulose acetate MIM membrane has the highest value compared to other variation membranes, because the cellulose acetate MIM membrane is rich in –OH (hydroxyl) groups so that it makes the membrane more hydrophilic. The percentage of cellulose acetate MIM membrane porosity test was 86.75%, the percentage of water absorption test was 91.09%, the highest flux test value of cellulose acetate MIM membrane with demineralized water solution was 5.78 L/m^2.hr. while the tensile test of the cellulose acetate NIM membrane was 12.141 N/mm^2. The increase in the percentage value of porosity is directly proportional to the percentage value of water absorption and flux, but inversely proportional to the results of the tensile test which has a lower Young's modulus value compared to cellulose.

Keywords: Cellulose, Cellulose Acetate, Hollow Fiber, MIM, Hemodialysis.

INTRODUCTION

One of the important roles of the kidneys is to excrete the residues of the body's metabolism, for example urea, uric acid, and creatinine. If these metabolic residues are allowed to accumulate, they can become toxic to the body, especially the kidneys. Thus, if the kidneys fail, this important role will cause problems.The results of metabolites such as urea and creatinine will be higher (Suryawan et al., 2017).

Based on data from the Ministry of Health for 2022, acute kidney failure in children in 2022 is the most common in Indonesia with a total of 118 deaths, which exceeds the number of deaths in Gambia which amounted to 50 deaths. Chronic kidney disease (CKD) is a threat to patients because of the high morbidity and lack of medical expenses (Azhar et al., 2021). Chronic kidney failure is a disorder that occurs in progressive and irreversible kidney function in which the body's ability to maintain fluid and electrolyte balance and excretion of metabolic waste is lost, causing uremia. (Djunaidi et al., 2021) and can cause complications and even kidney transplant if hemodialysis is not done.

Hemodialysis has a process related to the removal of metabolic residue particles in the artificial kidney. It takes place in a dialysis machine, in which the patient's blood is removed from the blood vessels and then cleaned through diffusion and ultrafiltration processes. Substances that are filtered in the form of water, ammonia, salt, urea, and creatinine. Dialysate solutions contain chemicals that are similar to those found in the body, such as acetate, acetic acid, and glucose (Raharjo et al., 2017). In hemodialysis, currently many use a membrane that functions as a separator for metabolic residues with the patient's blood which is then circulated itself.

The membrane in general, is defined as a semipermeable thin layer that has a function as a special filter that can separate the components of a mixture (Raharjo et al., 2017). According to (Raharjo et al., 2017) membranes have several advantages, namely: (i) they require a small amount of energy, which does not include changes in the molecular structure of the substance being separated; (ii) can be performed at room temperature; (iii) and does not require additional chemical substances during the separation process.

Physicochemical properties, such as porosity, hydrophilicity, hemocompatibility, and mechanical properties; then the morphology and surface of the membrane, such as the concentration of polymer, solvent, and additives in the hemodialysis membrane prepared with the polymer mixture must be good (Azhar et al., 2021). Most of the membranes used for hemodialysis use hollow fiber membranes, they are preferred compared to flat membranes, because they have a relatively small surface area. Meanwhile, hollow fiber membranes can provide better performance due to the larger flat surface area (Raharjo et al., 2017).

This study used Molecularly Imprinted Membrane (MIM) and Non-Imprinted Membrane (NIM). MIM is a membrane that has the ability to recognize molecules due to its template which is achieved through cross-linking between the functional polymer and the target molecule. MIM has several advantages, namely: high stability and specificity, the impression material has greater flexibility in choosing the appropriate functionality due to the availability of a large number of compounds that can be polymerized (Djunaidi et al., 2021). One of the polymers used for the preparation of hemodialysis membranes, namely cellulose and cellulose acetate which has the advantages of good toughness, biodegradability, sustainable characteristics, biocompatible, and cheap compared to other polymers (Azhar et al., 2021). Several previous researchers have developed hemodialysis membranes based on cellulose acetate and polysulfone using the phase inversion method, including studies on membrane porosity, hydrophilicity, and selectivity for uremic toxins such as urea and creatinine (Hayder et al., 2018).

The development of molecularly imprinted polymer (MIP) and molecularly imprinted membrane (MIM) technologies for hemodialysis has also been reported as a promising approach for selective removal of uremic toxins (Djunaidi et al., 2021; P. Fan & Wang, 2009a). Earlier foundational work by the research group demonstrated selective MIP synthesis for glucose using polyeugenol as a functional polymer (Djunaidi & Astuti, 2019), separation of metal mixtures using a novel eugenol-derived carrier by bulk liquid membrane (Djunaidi et al., 2017) and synthesis of Fe(III)-imprinted polyeugenol using PEGDE as a crosslinker for selective Fe(III) sorption (Djunaidi et al., 2015). Further advances include hollow fiber MIM membranes based on eugenol functionalized with di-(2-ethylhexyl) phosphoric acid (D2EHPA) as a hemodialysis candidate (Djunaidi et al., 2024), polysulfone-cellulose hollow fiber membranes with urea imprinting via varied crosslinkers (Djunaidi et al., 2026), and eugenol-based hollow fiber membranes for seawater desalination (Djunaidi et al., 2025).

EXPERIMENTAL SECTIONS

Materials

The materials used in this research were Cellulose (Sigma Aldrich), Cellulose Acetate (Sigma Aldrich), Polysulfone (PSF) (Sigma Aldrich), Poly (ethylene glycol) 6000 (Merck), N-Methyl-2-Pyrolidone (NMP) (Merck), NaOH pa (Merck), Urea (Merck), Creatinine (Merck), Vitamin B12 (Merck), 4-(Dimethylamin-Benzaldehyde) (Merck), Picric Acid (Merck), Na_2HPO_4 (Merck), NaH_2PO_4 (Merck), demineralized water (Brataco)

Instrumentation

The instrumentation used in this research were Equipment laboratory glassware (Pyrex and Herma), Analytical balance (Ohaus), Stirrer, Magnetic bar, pH meter (Senz pH), Casting machine, Caliper (Digital Caliper), UV-Vis Spectrophotometer (B-One), FTIR (Shimadzu Prestige 21 ASTM), HT-2402 universal testing machines, SEM-EDX.

Contacting Cellulose and Cellulose Acetate with Urea 1000 ppm

Cellulose and cellulose acetate are contacted with 1000 ppm urea which aims to insert the urea molecule (template) into the membrane. Contacting was carried out using a ratio of 1:20, namely between cellulose and cellulose acetate with a concentrated urea solution of 1000 ppm. A total of 1 gram of cellulose and cellulose acetate was added to 20 mL of 1000 ppm urea solution and then stirred using a stirrer for 24 hours in a tightly closed container, filtered, and dried at room temperature.

MIM (Molecularly Imprinted Membrane) Synthesis of Cellulose and Cellulose Acetate-Urea

Cellulose and cellulose acetate which have been contacted with urea concentration of 1000 ppm are added polysulfone (PSF) and Poly (ethylene glycol) 6000 (PEG 6000) with a ratio of 1:4:1 dissolved with N-Methyl-2-Pyrolidone (NMP) solvent and catalyst using 0.1% NaOH solution. A total of 0.833 grams of cellulose-urea powder, 3.333 grams of PSF, and 0.833 grams of PEG in 12 mL of NMP and 0.25 mL of 0.1 M NaOH solution in a two-neck flask was refluxed by heating at 90-100°C in a two-neck flask. The mixture was homogenized using a stirrer for 10 hours, then transferred to a 100 mL vial. After membrane spinning, the template (urea) must be removed from the membrane by a leaching process to create molecular recognition cavities. The membrane was soaked in a 0.1 M HCl solution for 24 hours with stirring to elute the urea template, then washed thoroughly with aquademin until the washing solution showed no absorbance at the urea detection wavelength (UV-Vis spectrophotometer). The complete removal of the template was confirmed by FTIR analysis, indicating the disappearance of the urea N-H stretching peak.

NIM (Non-Imprinted Membrane) Synthesis

The steps of NIM synthesis were carried out in the same way as MIM membrane synthesis, but cellulose and cellulose acetate were not brought into contact with 1000 ppm urea.

Hollow Fiber Membrane Spinning

The schematic diagram of the hollow fiber membrane spinning device is presented in **Figure 1**, which illustrates the main components: (1) the dope solution tank (Tube 1), (2) the bore fluid tank (Tube 2) containing distilled water as bore fluid, (3) the compressor connected via hose equipped with a flowmeter, (4) the spinneret (die) through which both solutions are co-extruded, (5) the air gap of 30 cm where initial solvent evaporation occurs, and (6) the coagulation bath filled with water at temperature below 50°C where solidification of the hollow fiber membrane takes place via non-solvent induced phase separation (NIPS). The solidified hollow fiber membrane is then collected on a take-up roll. The membrane dope solution was spun into hollow fiber membranes using a laboratory scale dry wet spinning apparatus via the non-solvent induced separation (NIPS) method.

Characterization of the Physical Properties of the Membrane

Characterization of the physical properties of the membrane includes SEM-EDX test, porosity test, absorption test, tensile test, and flux test. For SEM-EDX analysis, the membrane samples were freeze-fractured in liquid nitrogen to expose the cross-sectional morphology, then sputter-coated with gold prior to imaging. Membrane cross-sections and surface morphologies were observed at 200× and 3000× magnification, respectively, using a scanning electron microscope equipped with an energy-dispersive X-ray (EDX) detector to determine elemental composition. For the tensile test, membrane samples were cut into strips and subjected to uniaxial tensile loading using an HT-2402 universal testing machine at a constant crosshead speed of 10 mm/min. Young's modulus (MPa) was calculated from the initial linear region of the stress-strain curve.

RESULTS AND DISCUSSION

MIM synthesis

The synthesis of MIM (Molecularly Imprinted Membrane) involves precontacting the functional polymer with a template molecule in this case urea to create specific binding sites within the polymer matrix. After membrane fabrication, the template is removed by leaching with 0.1 M HCl for 24 hours, leaving complementary cavities that selectively recognize and transport the target molecule during hemodialysis application.

From the results of the FTIR analysis of Cellulose and Cellulose-Urea, analysis was carried out using the Fityk software in the range of wave numbers 1600-1700 cm^{-1}. This is to determine the peak deconvolution that occurs between cellulose and cellulose-urea which is shown in **Figure 2**. The results obtained after using the Fityk software on the FTIR results of cellulose show that there are 7 absorption peaks below the actual peak. This is possible because of the overlapping of these peaks. Allegedly, peak I at absorption of 1,611 cm^{-1} as an aromatic stretching vibration(C=C), peak II at absorption of 1,636 cm^{-1} as C=C stretching vibration (C=C), peak III at absorption of 1,656 cm^{-1}, peak IV at absorption of 1,673 cm -1, the V peak at 1,686 cm^{-1} absorption as a C=N stretching vibration, the VII peak at 1,648 cm^{-1} absorption as a C=N amide stretching vibration.

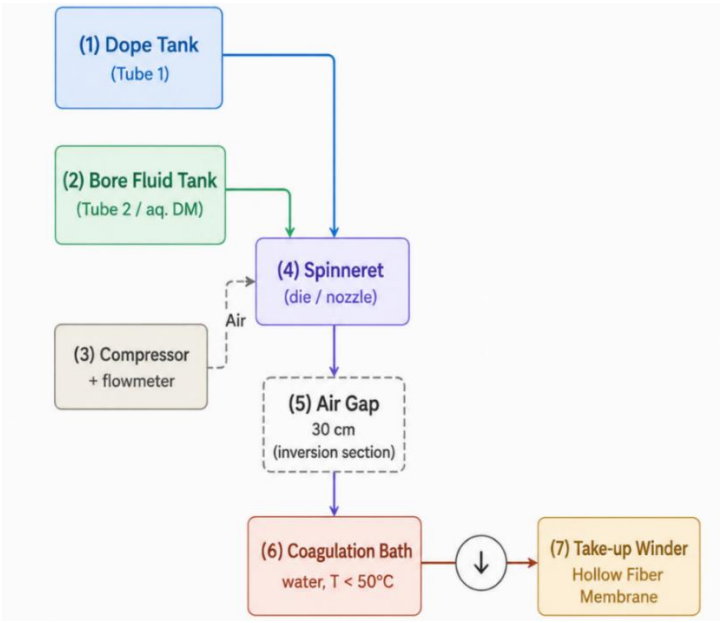

Figure 1. Schematic diagram of the hollow fiber membrane spinning device

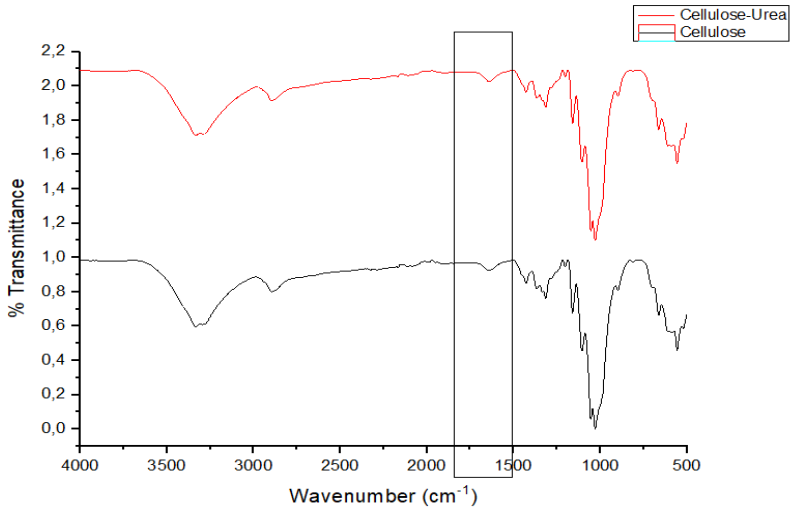

Figure 2. FTIR graphics of cellulose and cellulose-urea

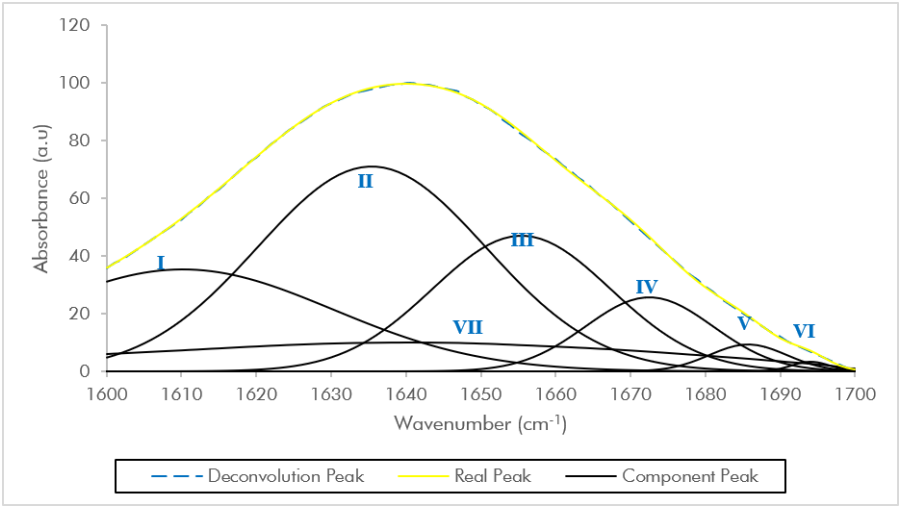

Figure 3. Cellulose fityk graphic

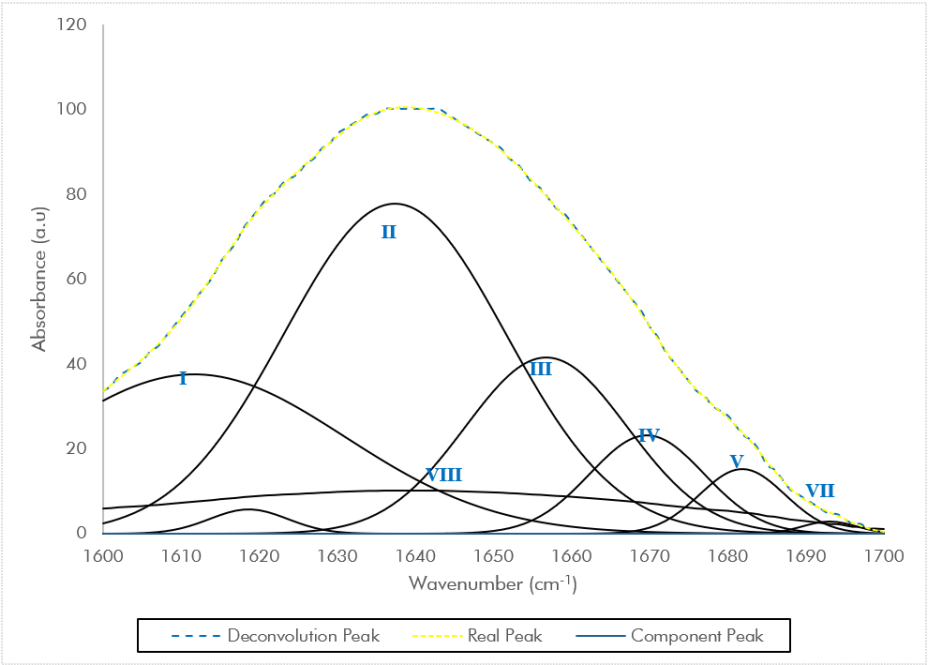

Figure 4. Graph of cellulose-urea Fityk

The results obtained after using the fityk software on the FTIR results of cellulose-urea, showed 8 absorption peaks. Allegedly, peak I at 1,611 cm^{-1} absorption as aromatic (C=C) absorption, peak II at 1,619 cm^{-1} absorption and peak III at 1,638 cm^{-1} absorption as NH absorption (Manivannan & Rajendran, 2011), peak IV at absorption of 1,658 cm^{-1}, peak V at absorption of 1,669 cm^{-1}, peak VI at absorption of 1,682 cm^{-1} as C=N absorption, peak VII at absorption of 1,693 cm^{-1} as absorption of carboxylic acid (C=O) , and peak VIII at 1,644 cm^{-1} absorption as amide absorption (C=O). Thus, the presence of peak II in the absorption analysis of urea-contacted cellulose concluded that the cellulose was successfully contacted with urea (template) through hydrogen bonding interactions, as illustrated in **Figure 5**.

The resulting weight of cellulose contacting was obtained at 11.859 grams. Furthermore, to measure the percentage of urea contacted on the polymer, namely cellulose, an analysis was carried out using a UV-Vis spectrophotometer of 1000 ppm urea solution before contacting and the filtrate after contacting. The results obtained showed that the amount of urea adsorbed on cellulose was 559.85 ppm with a percentage of 45.26%. The amount of urea that interacts with the polymer is one of the important things to determine the performance of the membrane later when applied to transport.

From the MIM synthesis, a white solution mixture was obtained with a thick physical solution. Research conducted by (Fan & Wang, 2009) that with increasing concentration of PSF, the membrane surface will thicken. The addition of PEG to the solution apart from being a crosslinker, also functions to improve the structural morphology and properties of the membrane (Fan & Wang, 2009). The number of compositions in the synthesis of cellulose-urea MIM aims to obtain the best membrane results in order to increase the ability of membrane transport. Approximate interactions between cellulose-urea, PEG, and polysulfone are shown in **Figure 6**.

The resulting weight of cellulose contacting was obtained at 17.153 grams. Furthermore, to measure the percentage of urea contacted on the polymer, namely cellulose acetate, an analysis was carried out using a UV-Vis spectrophotometer of 1000 ppm urea solution before contact and the filtrate after contact. The results obtained showed that the amount of urea adsorbed on cellulose acetate was 432.45 ppm with a percentage of 37.45%. The amount of urea that interacts with the polymer is one of the important things to determine the performance of the membrane later when applied to transport.

As a result of the MIM synthesis, a slightly clear white solution mixture was obtained with a thick physical solution. Research conducted by (Fan & Wang, 2009)that with increasing concentration of PSF, the membrane surface will thicken. The addition of PEG to the solution apart from being a crosslinker, also functions to improve the structural morphology and properties of the membrane (Fan & Wang, 2009). The number of compositions in the synthesis of cellulose acetate-urea MIM aims to obtain the best membrane results in order to increase the ability of membrane transport. Approximate interactions between cellulose acetate-urea, PEG, and polysulfone are shown in **Figure 9**.

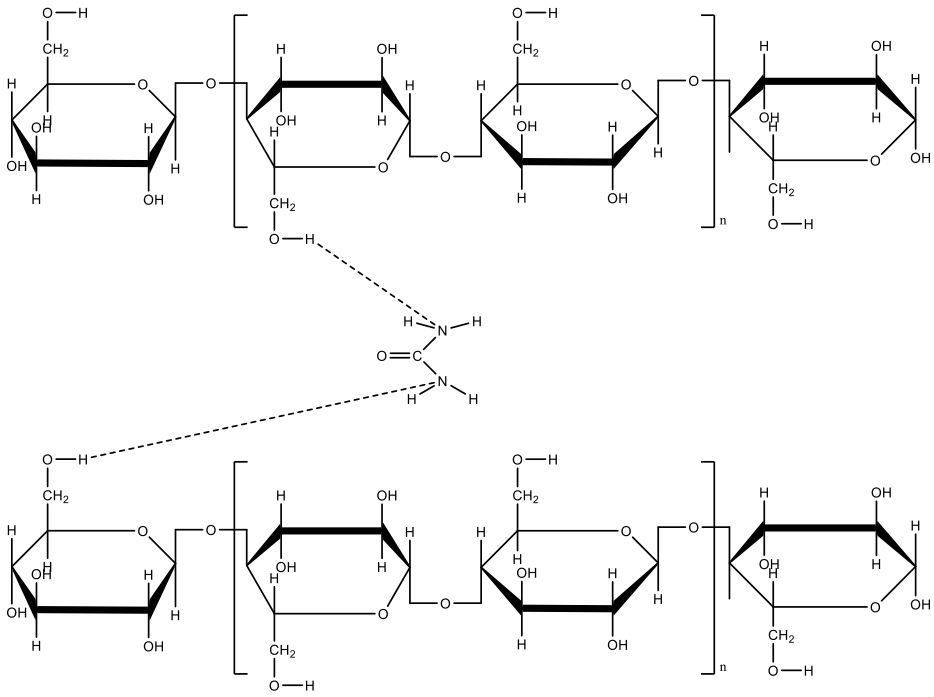

Figure 5. Estimated interaction of cellulose with urea

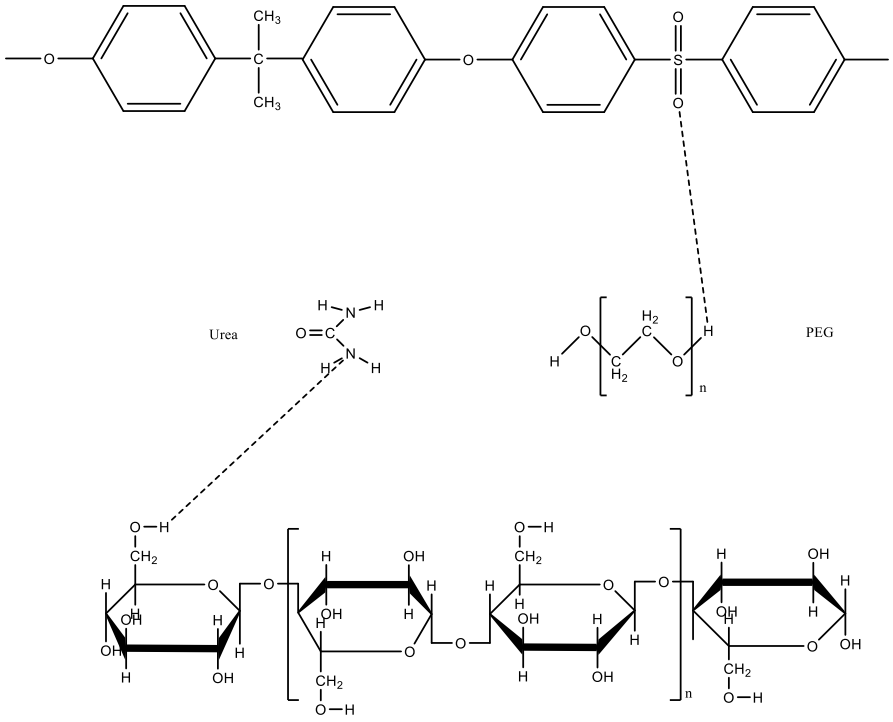

Figure 6. Estimates of cellulose-urea, PEG, and polysulfone interactions

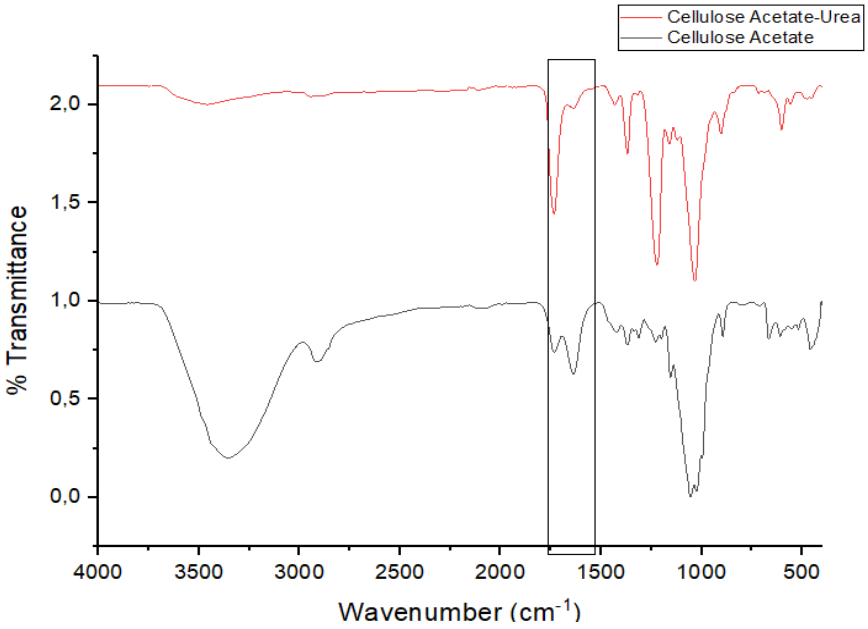

Figure 7. FTIR graph of cellulose acetate and cellulose acetate-urea

NIM synthesis

NIM is synthesized in the same way as MIM, but the functional polymers used are different. The functional polymers used in the synthesis of NIM are cellulose (C) and cellulose acetate (CA) which are not contacted with 1000 ppm urea solution (template). Approximate interactions between polysulfone, PEG and cellulose are depicted in the **Figure 10**. Then the approximate interaction between polysulfone, PEG and cellulose acetate is depicted in the **Figure 11**.

As a result of the synthesis of NIM cellulose and cellulose acetate, a white solution mixture was obtained with a thick physical solution. Research conducted by(P. Fan & Wang, 2009)that with increasing concentration of PSF, the membrane surface will thicken. The addition of PEG to the solution apart from being a crosslinker, also functions to improve the structural morphology and properties of the membrane (Fan & Wang, 2009). The number of compositions in the synthesis of NIM cellulose and cellulose acetate-urea aims to obtain the best membrane results in order to increase the adsorption capacity of the membrane.

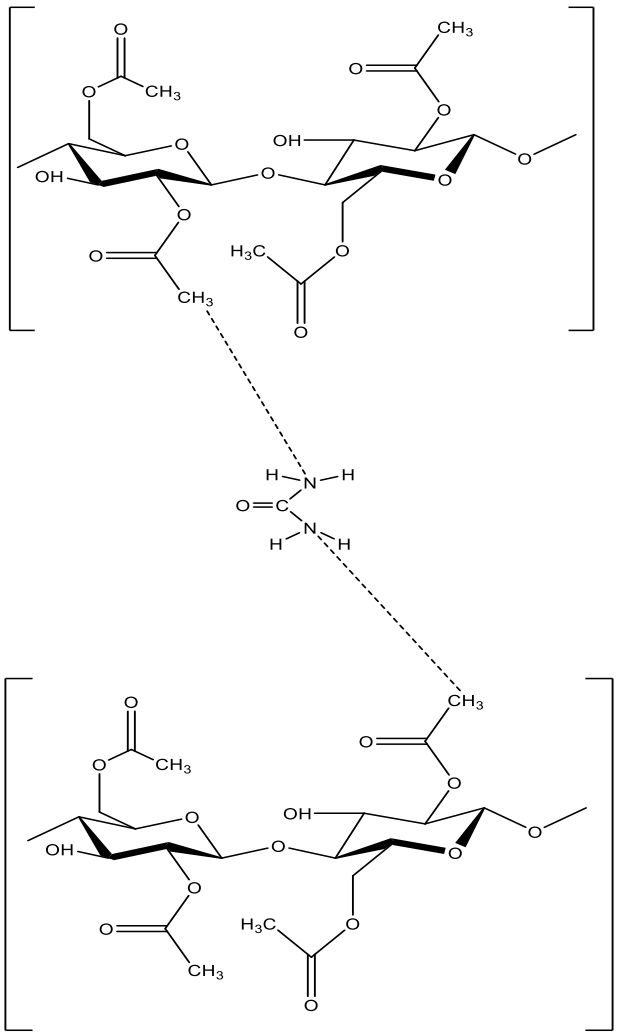

Figure 8. Estimated interaction of cellulose acetate with urea

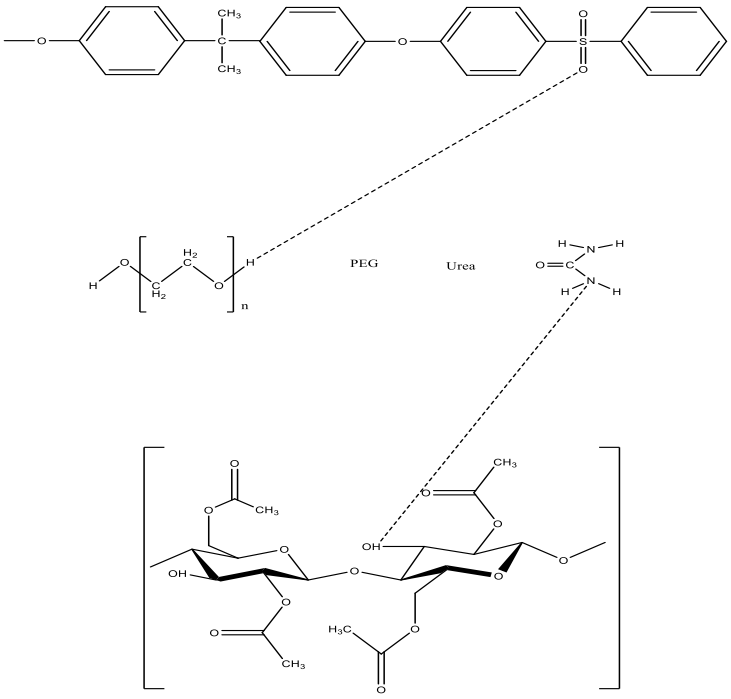

Figure 9. Estimates of cellulose-urea, PEG, and polysulfone interactions

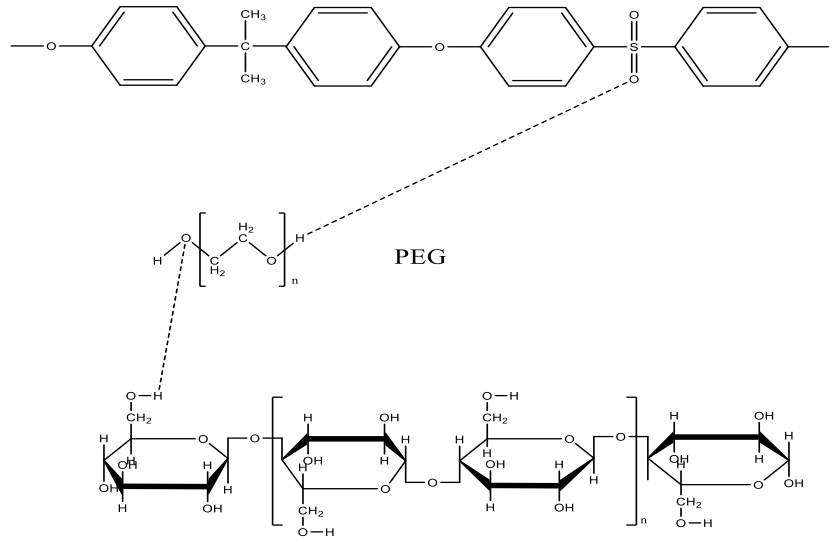

Figure 10. Estimated interactions of cellulose, PEG, and polysulfone

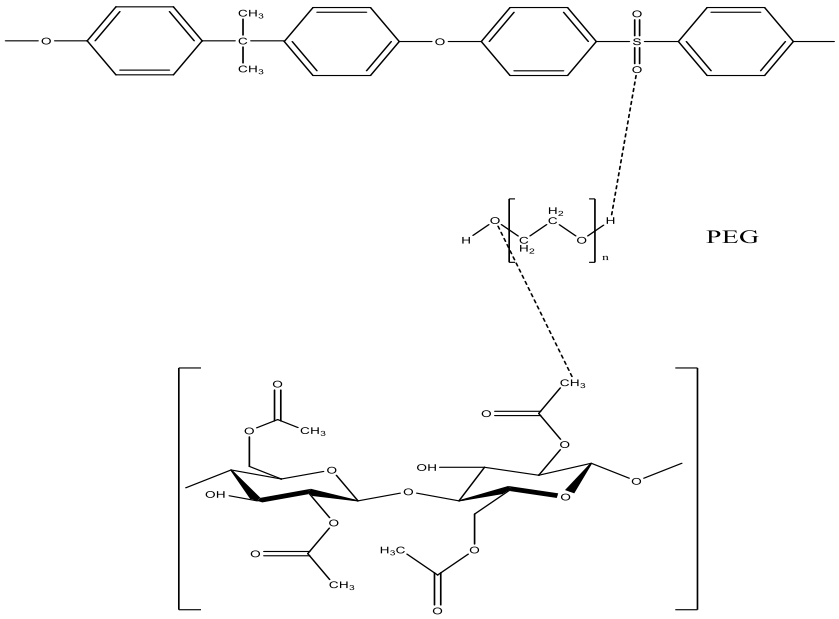

Figure 11. Estimated interactions of cellulose, PEG, and polysulfone

Characterization of the Physical Properties of the Membrane

SEM-EDX

SEM-EDX analysis was conducted to determine the morphology, pore size, surface, and elemental content of the membrane. SEM results show the effect of NIM membrane variation on membrane morphology with 200 times magnification shown in **Figure 12** and a cross section of the membrane with 3000 times magnification shown in **Figure 13**.

The figure shows that the cross-sectional results of NIM cellulose membrane are asymmetric, meaning that the membrane has a dense top layer and a sub-layer in the form of finger-like pores (Fathanah et al., 2021) and NIM cellulose acetate in the form of sponge-like pores. This can be attributed to the sponge-like pore shape, due to slow deposition (Kim et al., 2015). In addition, the addition of PEG functions as a pore-forming agent (Khayet et al., 2010), namely the greater the molecular weight of PEG, the larger the resulting pore size (Khoiroh et al., 2019) and a solution with a higher PEG content will produce an amorphous phase without eliminating the small crystalline phase, thus a membrane with better transport properties is obtained due to the presence of PEG (Kim et al., 2015). PEG in the membrane causes the bond between polymers to be weak. Its hydrophilic nature causes the solvent exchange process to be faster and the macrovoid size to be larger. In addition, when spinning the hollow fiber membrane, the membrane is immersed in a coagulation bath containing aquademin, making the membrane settle and pore formation occurs due to the weak solubility of polysulfone mixed with cellulose-cellulose acetate or NMP solvent exchange with water much faster to form finger-like macrovoids.

The figure shows that the morphological results of NIM cellulose acetate membrane have larger pores

and tend to be more tenuous than NIM cellulose. The more hydrophilic groups, the more permeate that can be passed by the membrane. Solutions that have a lower concentration of cellulose acetate have a lower viscosity value and a greater dissolving capacity (Fan et al., 2015).

The SEM results show the effect of MIM membrane variation on membrane morphology with a magnification of 200 times shown in **Figure 14** and a cross section of the membrane with a magnification of 3000 times shown in **Figure 15**.

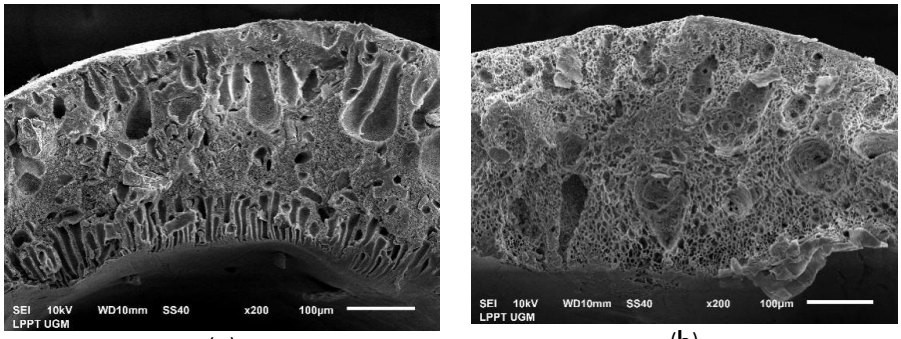

(**a**) (**b**)

Figure 12. SEM results of cross-section of NIM membrane (**a**) cellulose NIM (**b**) cellulose acetate NIM.

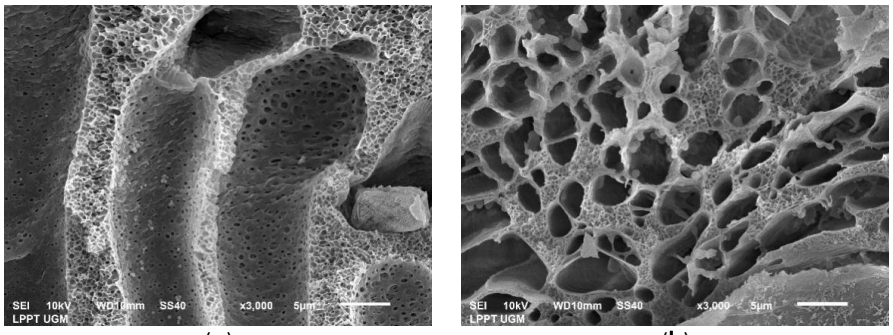

(**a**) (**b**)

Figure 13. SEM results of NIM membrane morphology (**a**) cellulose NIM (**b**) cellulose acetate NIM.

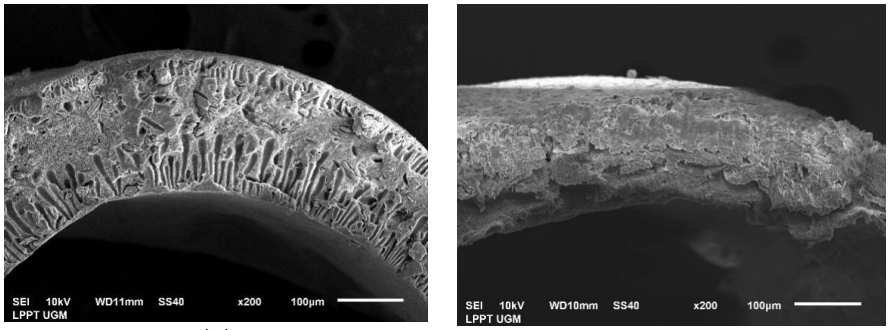

(**a**) (**b**)

Figure 14. SEM results of cross-section of MIM membrane (**a**) cellulose MIM (**b**) cellulose acetate MIM

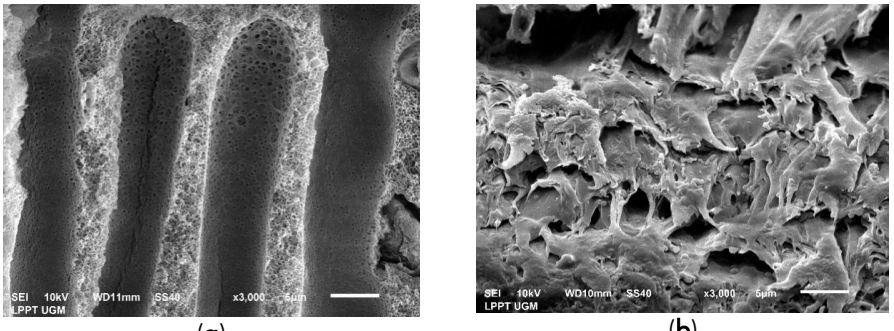

(**a**) (**b**)

Figure 15. SEM results of MIM membrane morphology (**a**) cellulose MIM (**b**) cellulose acetate MIM

In the **Figure 14**, it shows that the overall cross-sectional results of the membrane are asymmetric, meaning that the membrane has a dense top layer and a finger-like pore-shaped sub-layer (Fathanah et al., 2021). However, the pores in the cellulose acetate MIM membrane are not visible, due to its very fragile physical form, so that when cut, the SEM results of the cross-sectional shape and morphology of the membrane are not visible. In this case, the performance of the separation layer is caused by poor moulding of the hollow fibre membrane and sometimes the membrane structure is not easy to form (Fan et al., 2015).

In the **Figure 15** , it is possible that the morphological results of the cellulose acetate MIM membrane have larger pores and tend to be more tenuous than cellulose MIM. The more groups that are hydrophilic, the more permeate that can be passed by the membrane. In addition, immersion of the membrane in the coagulation bath during the dry wet spinning process promotes solvent non solvent exchange, resulting in large pore cavities. Complete removal of the urea template was confirmed by UV-Vis spectrophotometry (no absorbance at λ = 425 nm using Ehrlich reagent) and FTIR analysis (disappearance of N-H Stretching at ~3340 cm^{-1}). Polymer-urea hydrogen bonding between C=O and N-H groups of urea and -OH groups of cellulose/cellulose acetate is confirmed by FTIR deconvolution in **Figure 2-4**.

Membrane Porosity Test

The porosity test aims to quantify the void volume fraction of the membrane. Porosity (ε) was calculated using Equation (1): ε (%) = [(Ww – Wd) / (ρw × A × l)] × 100%, where Ww = wet membrane weight (g), Wd = dry membrane weight after oven-drying at 100°C (g), ρw = density of water (0.998 g/cm^3), A = membrane area (cm^2), l = membrane thickness (cm). Higher porosity values are directly related to greater water flux performance.

The figure shows that the MIM of cellulose acetate has the greatest percentage of porosity, which is 86.75%. This is possible due to the influence of the inclusion of the urea molecule, namely the –OH group which is hydrophilic which can make the membrane more hydrophilic. So that the phase inversion process in the solvent can facilitate the increase in membrane porosity.

Water Absorption Test

The water absorption test evaluates the membrane capacity to take up water, reflecting its hydrophilicity and available void space. Water uptake (WU) was calculated using Equation (2):

$$wu\ (\%) = \left[\frac{(Ww - Wd)}{Wd}\right] \times 100\%,$$

where Ww = weight of the wet membrane (g) and Wd = weight of the dry membrane (g). The water uptake results for each membrane variation are shown in **Figure 17**.

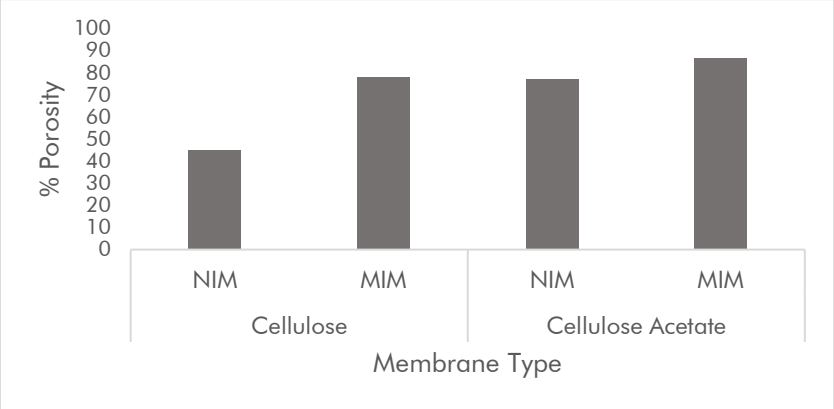

Figure 16. Membrane porosity chart

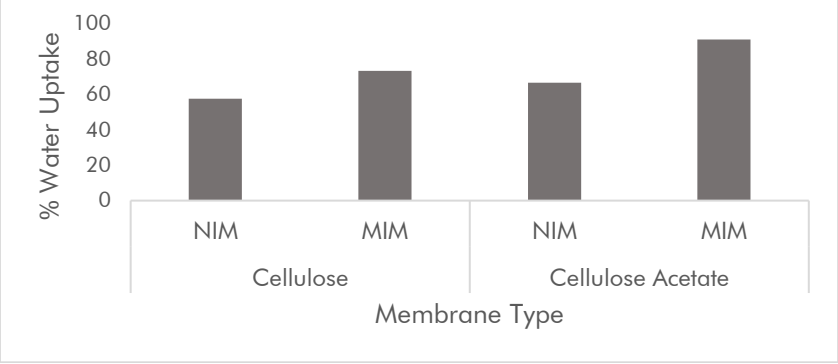

Figure 17. Membrane water absorption graph

The figure shows that the cellulose acetate MIM membrane has the greatest percentage of water absorption, which is 91.09%. This is due to the large number of –OH groups in cellulose acetate which are hydrophilic and it is possible that the influence of the inclusion of urea molecules, namely the –OH groups which are hydrophilic can make the membrane more hydrophilic. So as to be able to increase the hydrophilicity value of the membrane which can cause increased water absorption.

Flux Test

The flux test measures the volume of solution permeating through the membrane per unit area per unit time. Flux (J) was calculated using Equation (3): J (L/m²·hr) = $\frac{V}{A \times t}$, where V = volume of permeate collected (L), A = effective membrane area (m²), and t = time of permeation (hr). The feed solutions used were aquademin, urea, creatinine, and vitamin B12. The volume of the solution that drips or does not pass through the membrane is then calculated; the more feed solution that permeates, the larger and more numerous the pores in the membrane (Juniarzadinata, 2011).

The figure shows that the MIM cellulose membrane with aquademin solution has the largest flux value, namely, 3.74 L/m².hour, while the NIM cellulose membrane with vitamin B_{12} solution has the smallest flux value, namely, 0.04 L/m².hour. The MIM cellulose membrane with aquademin solution has the greatest flux value due to the presence of urea molecules in the membrane, namely the hydrophile -OH group, which can cause the membrane to be more hydrophilic so that the membrane has a tendency for liquids to enter the pores faster than membranes that are hydrophobic. In addition, due to the molecular weight of aquademin which is only 18 g/mol (Brewer & Peltzer, 2019), while the molecular weight of vitamin B_{12} is 1,355 g/mol (van de Lagemaat et al., 2019), so the molecular weight of aquademin is the smallest compared to other solutions, such as urea, creatinine, and vitamin B12. Then, the results of the flux value of MIM and NIM cellulose acetate membranes with various solutions are shown in **Figure 19**.

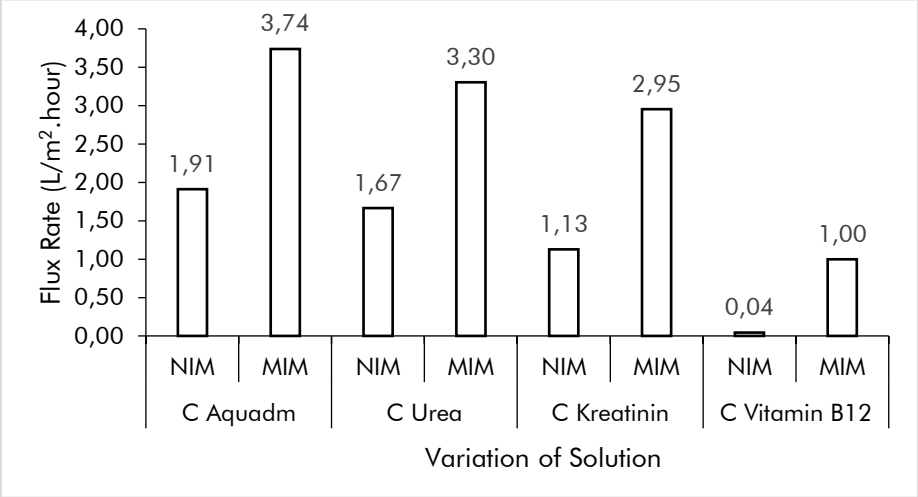

Figure 18. Graph of cellulose membrane flux test

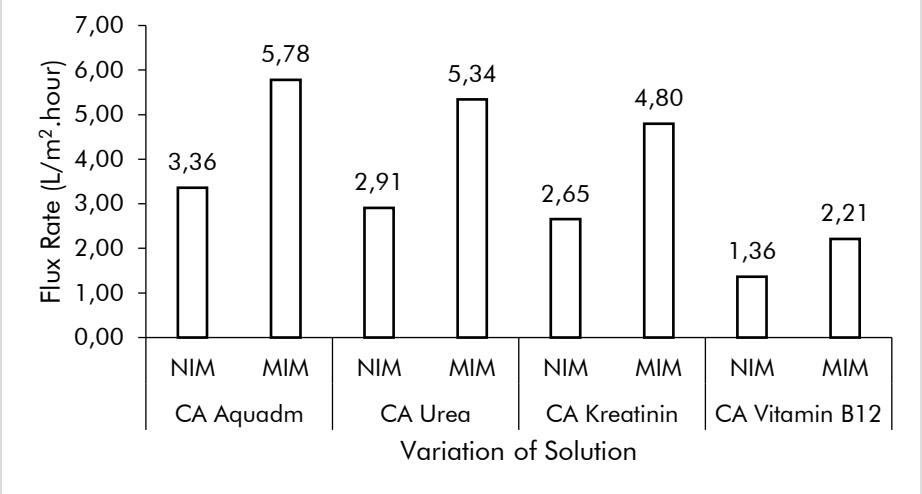

Figure 19. Graph of cellulose acetate membrane flux test

The **Figure 18** and **19** shows that the cellulose acetate MIM membrane with aquademin solution has the largest flux value, namely, 5.78 L/m^2.h, while the cellulose acetate NIM membrane with vitamin B_{12} solution has the smallest flux value, namely, 1.36 L/m^2.h. Due to the presence of acetate groups, namely —OH groups, on cellulose acetate and the influence of the entry of urea molecules, namely —NH groups, which are hydrophilic, the membrane is more hydrophilic.

When compared between MIM cellulose and MIM cellulose acetate, each of which uses aquademin solution, the one with the largest flux value is the MIM cellulose acetate membrane. This is due to the presence of acetate groups on cellulose acetate which makes the MIM cellulose acetate membrane more hydrophilic than MIM cellulose.

CONCLUSIONS

The performance of the cellulose acetate MIM membrane in this study, with a porosity of 86.75%, water absorption of 91.09%, and flux of 5.78 L/m^2·h, demonstrates superior hydrophilicity compared to previously reported polysulfone-based hollow fiber MIM membranes, where flux values were lower due to the absence of acetate functional groups. This finding is consistent with earlier reported that the incorporation of hydrophilic groups in cellulose acetate composite membranes significantly enhances water permeability and selectivity for uremic toxins. Furthermore, the urea-imprinted cavity formation confirmed by FTIR deconvolution provides evidence of a more selective transport mechanism compared to non-imprinted polysulfone membranes reported by (P. Fan & Wang, 2009), supporting the effectiveness of the molecular imprinting strategy for hemodialysis applications.

In this study, the hollow fiber membrane was fabricated using a dry wet spinning apparatus via the non solvent induced phase separation (NIPS) method. The porosity test, water absorption test, and flux test on the cellulose acetate MIM membrane had the highest values compared to other variation membranes. This is because the cellulose acetate MIM membrane is rich in –OH (hydroxyl) groups, making the membrane more hydrophilic. The increase in the percentage value of porosity is directly proportional to the percentage value of water absorption and flux, but inversely proportional to the results of the tensile test which has a low Young's modulus value compared to cellulose.

ACKNOWLEDGEMENTS

The authors would like to thank Diponegoro University and DRPM Ministry of Research and Technology/National Research and Innovation Agency for the research project entitled **Hollow Fiber Imprinted Membranes Cellulose Acetate Based For Hemodialysis** Based on assignment letter Directorate of Research and Community Service Deputy for Research and Development Strengthening Ministry of Research and Technology / National Research and Innovation Agency SPK Number : 569-99 / UN7.D2 / PP / VII / 2022.

REFERENCES

Azhar, O., Jahan, Z., Sher, F., Niazi, M. B. K., Kakar, S. J., & Shahid, M. (2021). Cellulose Acetate-Polyvinyl Alcohol Blend Hemodialysis Membranes Integrated with Dialysis Performance and High Biocompatibility. *Materials Science and Engineering*, *126*(April). https://doi.org/10.1016/j.msec.2021.112127

Brewer, P. G., & Peltzer, E. T. (2019). The Molecular Basis for the Heat Capacity and Thermal Expansion of Natural Waters. *Geophysical Research Letters*, *46*(22), 13227–13233. https://doi.org/10.1029/2019GL085117

C. Djunaidi, M., & Astuti, Y. (2019). Synthesis, Characterization and Selectivity of Molecularly Imprinted Polymer (MIP) Glucose Using Polyeugenol as a Functional Polyme. *Rasayan Journal of Chemistry*, *12*(02), 809–821. https://doi.org/10.31788/RJC.2019.1225120

Djunaidi, M. C., Febriola, N. A., & Haris, A. (2021). Molecularly Imprinted Membrane for Transport of Urea, Creatinine, and Vitamin B12 as A Hemodialysis Candidate Membrane. *Open Chemistry*, *19*(1), 806–817. https://doi.org/10.1515/chem-2021-0069

Djunaidi, M. C., Khabibi, & Ulumudin, I. (2017). Separation of Cu^{2+} , Cd^{2+} and Cr^{3+} in a Mixture Solution Using a Novel Carrier Poly(Methyl Thiazoleethyl Eugenoxy Acetate) with BLM (Bulk Liquid Membrane). *IOP Conference Series: Materials Science and Engineering*, *172*, 012032. https://doi.org/10.1088/1757-899X/172/1/012032

Djunaidi, M. C., Khusna, L., Maharani, N. D., Widodo, D. S., Khabibi, Muhtar, H., Susanto, H., & Filardli, A. M. I. (2026). In situ synthesis of urea printed polysulfone-cellulose hollow fiber membranes with crosslinker variations as hemodialysis membrane candidates. *Materials Chemistry and Physics*, *357*, 132393. https://doi.org/10.1016/j.matchemphys.2026.132393

Djunaidi, M. C., Maharani, N. D., Khabibi, K., Susanto, H., & Filardli, A. M. I. (2025). The Desalination of Seawater from Jepara Beach uses Hollow Fiber Imprinted Membrane-Based Eugenol. *Molekul*, *20*(1), 9. https://doi.org/10.20884/1.jm.2025.20.1.7836

Djunaidi, M. C., Maharani, N. D., Pardoyo, P., & Raharjo, Y. (2024). Hollow Fiber Hemodialysis Imprinted Membrane Based on Eugenol for Human Blood Filter. *Indonesian Journal of*

Chemistry, *24*(5), 1253. https://doi.org/10.22146/ijc.83065

Djunaidi, M., Siswanta, D., & Jumina, J. (2015). Eluent Influences on Synthesis of Fe(III)-imprinted Polyeugenol using Polyethylene Glycol Diglycidilether (PEGDE) as Cross-linking Agent and its application as Fe(III) sorbent. *Oriental Journal of Chemistry*, *31*(4), 2223–2229. https://doi.org/10.13005/ojc/310447

Fan, P., & Wang, B. (2009). Preparation of molecularly imprinted polymer membrane with blending trimethoprim-MIP and polysulfone and its transport properties. *Korean Journal of Chemical Engineering*, *26*(6), 1813–1820. https://doi.org/10.1007/s11814-009-0256-x

Fan, Z., Xiao, C., Liu, H., & Huang, Q. (2015). Preparation and Performance of Homogeneous Braid Reinforced Cellulose Acetate Hollow Fiber Membranes. *Cellulose*, *22*(1), 695–707. https://doi.org/10.1007/s10570-014-0466-1

Fathanah, U., Lubis, M. R., Mahyuddin, Z., Muchtar, S., Yusuf, M., Rosnelly, C. M., Mulyati, S., Hazliani, R., Rahmanda, D., Kamaruzzaman, S., & Busthan, M. (2021). Sintesis, Karakterisasi dan Kinerja Membran Hidrofobik Menggunakan Polyvinyl Pyrrolidone (PVP) sebagai Aditif. *ALCHEMY Jurnal Penelitian Kimia*, *17*(2), 140. https://doi.org/10.20961/alchemy.17.2.48435.140-150

Hayder, A., Hussain, A., Khan, A. N., & Waheed, H. (2018). Fabrication and characterization of cellulose acetate/hydroxyapatite composite membranes for the solute separations in Hemodialysis. *Polymer Bulletin*, *75*(3), 1197–1210. https://doi.org/10.1007/s00289-017-2084-1

Juniarzadinata, R. (2011). *Kajian struktur dan uji fluks membran polisulfon dengan metode inversi fasa* [Undergraduate thesis]. Institut Pertanian Bogor.

Khayet, M., Cojocaru, C., & García-Payo, M. C. (2010). Experimental Design and Optimization of Asymmetric Flat-Sheet Membranes Prepared for Direct Contact Membrane Distillation. *Journal of Membrane Science*, *351*(1–2), 234–245. https://doi.org/10.1016/j.memsci.2010.01.057

Khoiroh, N., Utomo, W. P., & Fansuri, H. (2019). Fabrikasi Membran Asimetris La0, 7Sr0, 3Co0, 2Fe0, 8O3-δ (LSCF 7328) dengan Penambahan Aditif Polietilen Glikol (PEG). *Jurnal Sains Dan Seni ITS*, *7*(2). https://doi.org/10.12962/j23373520.v7i2.36795

Kim, K., Ingole, P. G., Yun, S., Choi, W., Kim, J., & Lee, H. (2015). Water Vapor Removal Using CA/PEG Blending Materials Coated Hollow Fiber Membrane. *Journal of Chemical Technology and Biotechnology*, *90*(6), 1117–1123. https://doi.org/10.1002/jctb.4421

Manivannan, M., & Rajendran, S. (2011). Investigation of Inhibitive Action of Urea- Zn 2 + System in the Corrosion Control of. *International Journal of Engineering Science and Technology*, *3*(11), 8048–8060.

Raharjo, Y., Wafiroh, S., Nayla, M., Yuliana, V., & Fahmi, M. Z. (2017). Primary Study of Cellulose Acetate Hollow Fiber as a Green Membrane Applied to Hemodialysis. *Journal of Chemical Technology and Metallurgy*, *52*(6), 1021–1026.

Suryawan, D. G. A., Arjani, I. A. M. S., & Sudarmanto, I. G. (2017). Gambaran Kadar Ureum Dan Kreatinin Serum Pada Pasien Gagal Ginjal Kronis (Ggk) Yang Menjalani Terapi Hemodialisis Di Rsud Sanjiwani Gianyar. *Meditory : The Journal of Medical Laboratory*, *4*(2), 145–153. https://doi.org/10.33992/m.v4i2.64

van de Lagemaat, E. E., de Groot, L. C. P. G. M., & van den Heuvel, E. G. H. M. (2019). Vitamin B12 in Relation to Oxidative Stress: A Systematic Review. *Nutrients*, *11*(2). https://doi.org/10.3390/nu11020482